Jeffery Slip Fluid Flow with the Magnetic Dipole Effect Over a Melting or Permeable Linearly Stretching Sheet

Original Paper Published: 08 December 2023

Volume 10, article number 5, (2024) Cite this article

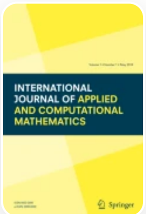

Amit Parmar

Department of Mathematics, Arya College of Engineering, and I.T, Jaipur, India

Contact Amit Parmar

View author publications

You can also search for this author in PubMed | Google Scholar

Krishna Agarwal, Randhir Singh Baghel, Amit…

Abstract

The magnetic dipole effect has garnered significant attention in recent years due to its potential impact on fluid flow phenomena. Researchers have explored its applications in areas such as microfluidics, nano-fluidics, additive manufacturing, drug delivery systems, magnetic resonance imaging, and hyperthermia treatments. The objectives of this research are twofold: first, to investigate the fundamental mechanisms and behaviors of Jeffery fluid flow under the influence of a magnetic dipole and slip effect; and second, to explore heat transport under the influence of melting effect and explore implications of this effect in various fields. Here we consider two different types of surface of fluid flow namely melting surface and permeable surface. By using the well-known similarity transformation, formulated flow equations are converted into OD equations and solved numerically using R–K 4th order with shooting techniques in Matlab. Graphical representations are used to show how different physical characteristics affect velocity and temperature profiles. The findings demonstrate that the velocity profile increases over a range of Deborah numbers (\(\gamma_{1}\)), whereas the temperature profile exhibits the opposite behavior. Velocity profile gets cut down for diverse values of ferromagnetic interaction parameter (\(\beta\)) but on the other hand temperature profile accelerates. The investigation also revealed that the viscous dissipation parameter λ had counterintuitive effects on the thermal profile. Deborah numbers \(\gamma_{1}\) on velocity \(f^{\prime } \left(\eta \right)\), with temperature \(\theta \left(\eta \right)\) profile. Whenever values \(\gamma_{1}\) get increased the velocity gets enhanced but alternatively temperature profile gets cut down. In this article, we find the tabulated form the numerical values of skin friction coefficient, Nusselt number in PST is given for numerical solution on melting surface case and without melting case for various values of the physical parameter. The graphically results show that the melting surface influence more than permeable surface.

Introduction

Non-Newtonian fluid flow stands up in many divisions of chemical and material processing engineering. There are various types of non-Newton fluids like Viscoelastic fluid, couple stress fluid, micropolar fluid power-law fluid, etc. In addition to these, there is another non-Newtonian model called the Jeffery fluid model.The stress relaxation feature of non-Newtonian fluids, which the typical viscous fluid model cannot represent, may be described using the Jeffrey fluid model. The framework of Jeffrey fluid may adequately explain a type of non-Newtonian fluids with different temporal scales for memories, also known as the relaxing period. The Couette and Poiseuille flows of a Jeffrey fluid under slip boundary conditions were the subject of an investigation by Ramesh [1] into the effects of viscous dissipation and Joule heating. Abbasi et al. [2] explained the interaction between Jeffrey nanofluid's mixed convection flow, thermal radiation, and double stratification. Shehzad et al. [3] investigated Jeffrey nanofluid thermally radiative three-dimensional flow with internal heat generation and field of magneticAccurate analytical solutions for the transport of heat and flow on a stretching/shrinking sheet close to the stagnation point in a Jeffrey fluid were provided by Turkyilmazoglu et al. [4]. Ellahi et al. [5, 6] examined the effect Bloodstream of Jeffrey liquid in a catheterized tightened supply route with the nanomaterials suspended and also investigated the Peristaltic transport of Jeffrey fluid in a rectangular tube. Hayat et al. [7] investigated the erratic flow as well as heat transfer of the Jeffrey fluid around a stretched sheet. Ahmed et al. [8] studied the convective heat transfer of the MHD Jeffrey fluid around a stretched sheet.

A model of electrically conducting fluids known as magnetohydrodynamics (MHD), sometimes known as magneto-fluid dynamics or hydromagnetics, considers all interpenetrating particle species as a single continuous medium. It has supplications in a deep range of regulations, involving geophysics, astronomy, and engineering, and is principally focused on the lower-frequency, wide range on the scale, magnetic behavior in plasmas and liquid metals. Ogulu et al. [9] modeling of pulsatile blood flow in a homogenous porous bed with a consistent magnetic field with time-varying suction was conducted. Alam et al. [10] look into the blood flow and the transfer of heat using gold nanoparticles around a stretched sheet when a magnetic dipole is present. In the situation of an unstable flow, Seddeek [11] investigated the outcomes of radiation together with changing viscosity on an MHD-free convection flow across a leveled plate with a semi-infinite length and an aligned magnetic field. Precise logical solutions for the heat and mass transfer of MHD slip flow in nanofluids were discovered by Turkyilmazoglu [12]. The outcomes of heat radiation, suction/blowing, and slide-on boundary layer flow of magnetohydrodynamics across an exponentially stretched sheet were looked over by Mukhopadhyay [13]. Raptis et al. [14] describe the outcomes of heat radiation on MHD flow. Iyoko et al. [15] Investigation of magnetic dipole and thermal radiation effects on Jeffery flow/heat transfer across a strain plate by suction/injection.

The procedure of melting is commonly utilized in machinery such as metal casting, laser manufacturing, wandering freezing, soil melting, rivers and lakes, etc. Singh et al. [16] looked into the effects of melting heat transfer in boundary layer stagnation point flow of MHD micro-polar fluid towards a stretching/shrinking surface. By employing carbon nanotubes, Hayat et al. [17] inspected the numerical analysis for melting heat transmission and homogeneous heterogeneous reactions in flow. Melting heat transfer in continuous laminar flow across a flat plate was given by Epstein et al. [18]. Melting heat transfer in constant laminar flow around a moving surface was given by Ishak et al. [19]. In a micropolar fluid, Yacob et al. [20] investigated the impression of melting heat transfer in boundary layer stagnation-point flow in the direction of a stretching/shrinking sheet. Olkha and Dadheech [21, 22] discussed entropy analysis for MHD flow for different non-Newtonian fluids caused by a stretching sheet with melting and slip effects. Dadheech et al. [23] investigated MHD flow for Casson fluid caused by a stretching sheet with melting and slip effects. Dadheech et al. [24] discussed entropy analysis for Williamson fluid caused by a vertical plate with Cattaneo-Christov heat flux and slip effect.

Although a fluid typically sticks to solid boundaries (has no slip), there are several circumstances in which this is not the case. For instance, suspensions, polymer melts, emulsions, and many other non-Newtonian fluids frequently show macroscopic wall slips. These fluids with boundary slip have uses in cleaning interior cavities, prosthetic heart valves, and several other technical operations. The slip effect on non-Newtonian fluid flows was investigated byLabropulu et al. [25]. Ali et al. [26] inspected slip effects in viscoelastic fluid flow caused by an oscillatory stretched sheet through a porous medium. Govindarajan et al. [27] discussed slip as well as mass transport effects in a vertical channel under consideration of heat source and radiation. The slip flow of Maxwell fluid past a non-linearly stretchy surface was examined by Dawar et al. [28]. Similar work has been studied by Dadheech et al. [29], Olkha et al. [30].

In light of the provided literature research, we have noted that there are just a few investigations on Jeffery fluid flow with magnetic dipole effect. The main objective of the current study is to determine flow behavior and heat transfer of Jeffery fluid flow with magnetic dipole effect. The novelty of the presented work is increased by substantial validating slip effects with radiation and heat source effects. The examinations furnished in the given article can be further utilized to make investigations in microfluidics, biomedical engineering, industrial processes (e.g., polymer manufacturing), and geophysics/astrophysics. It helps in the manipulation of micro-objects, drug delivery systems, process optimization, and understanding of magnetized fluids in Earth's core and stellar interiors. The work provided in the study has not yet been disseminated, to the best of the author's knowledge.

Mathematical Formulation

Jeffery flow with the magnetic dipole field, magnetic scalar potential is taken as

$$ \phi = \frac{\gamma }{2\pi }\left({\frac{x}{{x^{2} + (y + a)^{2} }}} \right)\,, $$

(1)

Here γ is the magnetic field strength, the component of x and y axis direction of the magnetic field are H_{x} and H_{y}.

$$ H_{x} = - \frac{\partial \phi }{{\partial x}} = \frac{\gamma }{2\pi }\left({\frac{{x^{2} - (y + a)^{2} }}{{(x^{2} + (y + a)^{2})^{2} }}} \right)\,, $$

(2)

$$ H_{y} = - \frac{\partial \phi }{{\partial y}} = \frac{\gamma }{2\pi }\left({\frac{2x(y + a)}{{(x^{2} + (y + a)^{2})^{2} }}} \right)\,, $$

(3)

The resultant magnitude H of the magnetic field intensity is

$$ H_{y} = \left[{\left({\frac{\partial \phi }{{\partial x}}} \right)^{2} + \left({\frac{\partial \phi }{{\partial y}}} \right)^{2} } \right]^{\frac{1}{2}} \,, $$

(4)

$$ \frac{\partial H}{{\partial x}} = - \frac{\gamma }{2\pi }\left({\frac{2x}{{(y + a)^{4} }}} \right)\,, $$

(5)

$$ \frac{\partial H}{{\partial y}} = - \frac{\gamma }{2\pi }\left({\frac{ - 2}{{(y + a)^{3} }} + \frac{{4x^{2} }}{{(y + a)^{5} }}} \right)\,, $$

(6)

Magnetization M could be a "linear function of temperature",

$$ M = K^{*} \left[{T_{c} - T} \right]\,\,, $$

Let us assume the steady 2-D flow passing through a stretchy surface shown schematically in Fig. 1. By applying two equal and opposite forces along the x-axis, the sheet being stretched is related to how far it is from the fixed origin at x = 0. Thus, only the moving sheet is responsible for the resultant motion of the otherwise quiescent fluid. A magnetic dipole is found some distance below the surface, while an incompressible, viscous, and electrically non-conducting ferrofluid is limited to the half-space y > 0 over the sheet. The dipole, whose center lies on the y-axis a distance below the x-axis and whose magnetic field points in the positive x-direction, rises to a magnetic area of sufficient strength to saturate the ferrofluid. The stretching sheet is kept at a constant temperature T_{w} lower than the Curie temperature T_{c}, while the fluid components are far off from the surface which is presumed to be at temperature $T_{\infty } = T_{c}$ and, hence, it is powerlessto be magnetized until they start to cool upon entering the thermal boundary layer closest to the surface.

Fig. 1

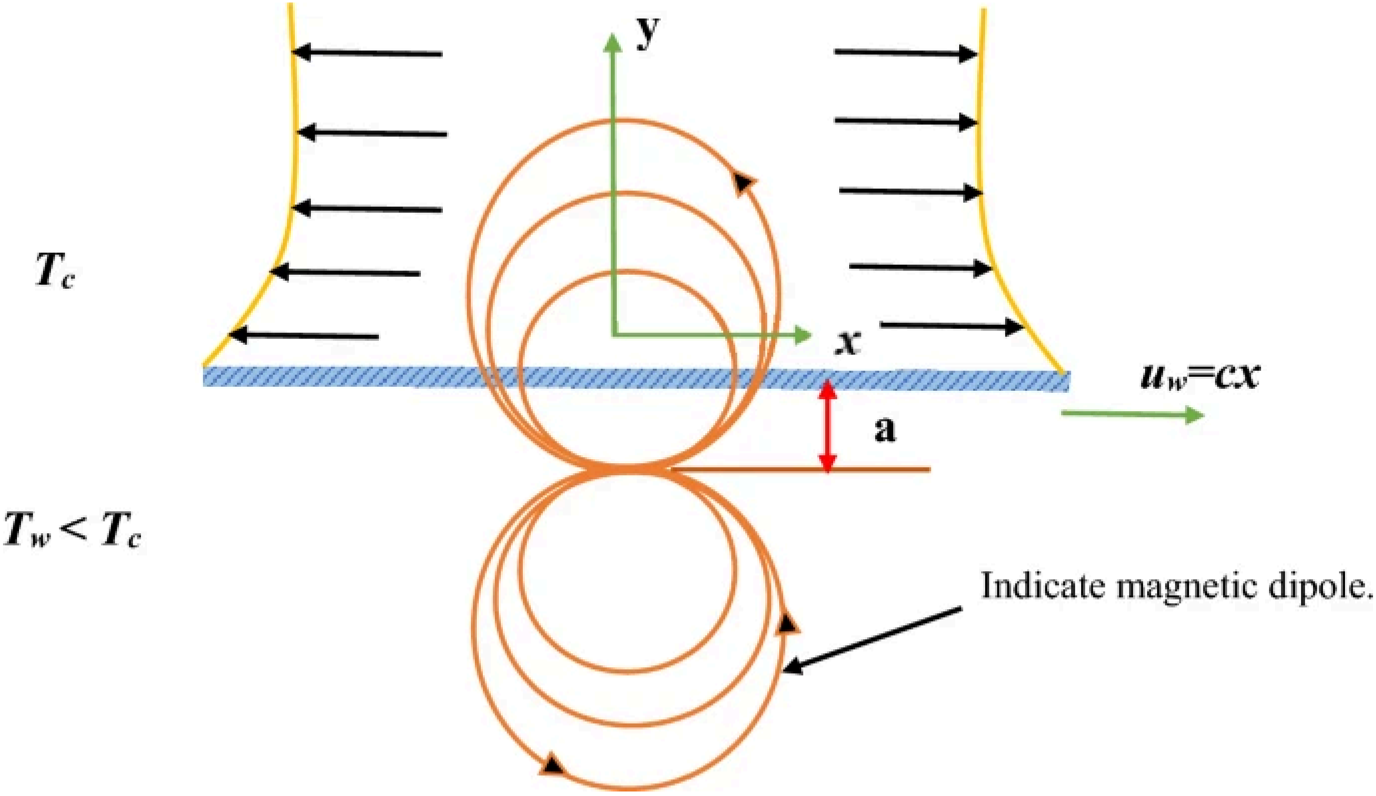

The geometry of the problem

The required equations for the Jeffrey model are written as

$$ \tau = pI + \kappa $$

(7)

$$ \kappa = \frac{\mu }{{1 + \lambda_{1} }}\left[{R_{1} + \lambda_{1} \left({\frac{{\partial R_{1} }}{\partial t} + V.\nabla } \right)R_{1} } \right] $$

(8)

$$ R_{1} = (\nabla V) + (\nabla V)^{\prime } $$

(9)

"Cauchy stress tensor:τ,extra stress tensor:κ, and the following terms are defined above paragraph.

Using the continuity, momentum, temperature equations, and the boundary conditions"

$$ \frac{\partial u}{{\partial x}} + \frac{\partial u}{{\partial y}} = 0 $$

(10)

$$ u\frac{\partial u}{{\partial x}} + v\frac{\partial u}{{\partial y}} = \frac{{\mu_{0} }}{\rho }M\frac{\partial H}{{\partial x}} + \frac{\nu }{{1 + \lambda_{2} }}\left[{\frac{{\partial^{2} u}}{{\partial y^{2} }} + \lambda_{1} \left({u\frac{{\partial^{2} u}}{\partial x\partial y} + v\frac{{\partial^{3} u}}{{\partial y^{3} }} - \frac{\partial u}{{\partial x}}\frac{{\partial^{2} u}}{{\partial y^{2} }} + \frac{\partial u}{{\partial y}}\frac{{\partial^{2} u}}{\partial x\partial y}} \right)} \right] + g\beta^{*} (T_{c} - T) $$

(11)

$$ u\frac{\partial T}{{\partial x}} + v\frac{\partial T}{{\partial y}} + \frac{{\mu_{0} }}{{\rho C_{p} }}T\frac{\partial H}{{\partial T}} = \frac{k}{{\rho C_{p} }}\frac{{\partial^{2} T}}{{\partial y^{2} }} + \frac{\mu }{{\rho C_{p} }}\left({\frac{\partial u}{{\partial y}}} \right)^{2} + \frac{2\mu }{{\rho C_{p} }}\left({\frac{\partial v}{{\partial y}}} \right)^{2} - \frac{1}{{\rho C_{p} }}\frac{{\partial q_{r} }}{\partial y} + \frac{{Q*(T_{c} - T)}}{{\rho C_{p} }} $$

(12)

where \(u(x,y)\) and \(v(x,y)\) are the "horizontal and vertical velocity components."

Following Rosselandestimate \(q_{r}\), the radiation heat flux is given \(q_{r} = - \left({\frac{4\sigma }{{3k^{*} }}} \right)\frac{{\partial T^{4} }}{\partial y}\), expanding T^4, in a Taylor series about \(T_{\infty }\),on neglecting higher order term and \(k*\): thermal radiation parameter, we get

$$ \begin{aligned} T^{4} & \approx T_{\infty }^{4} + 4T_{\infty }^{3} T - 4T_{\infty }^{3} T_{\infty } \\ \frac{{\partial q_{r} }}{\partial y} & = \frac{\partial }{\partial y}\left({\frac{ - 4\sigma }{{3k^{*} }}\frac{{\partial T^{4} }}{\partial y}} \right) = \frac{\partial }{\partial y}\left({\frac{ - 4\sigma }{{3k^{*} }}\frac{{\partial (T_{\infty }^{4} + 4T_{\infty }^{3} T - 4T_{\infty }^{3} T_{\infty })}}{\partial y}} \right) =

\frac{{ - 16\sigma T_{\infty }^{3} }}{{3k^{*} }}\frac{{\partial^{2} T}}{{\partial y^{2} }} \\ \end{aligned} $$

Following boundary conditions for PST and PHF cases are given below:

$$ \begin{aligned} & u = (u_{w} = cx) + L_{1} \frac{\partial u}{{\partial y}},\quad v = - v_{w} + \frac{k}{{\rho \left[{\beta + c_{s} (T_{m} - T_{0})} \right]}}\frac{\partial T}{{\partial y}}\quad {\text{at}}\quad y = 0 \\ & u \to 0,\quad \frac{\partial u}{{\partial y}} \to 0\quad {\text{at}}\quad y = \infty \\ \end{aligned} $$

$$ \begin{array}{*{20}l} {T = T_{w} = T_{c} - A\left(\frac{x}{l} \right)^{2} \;for\;PST} \hfill & {at\;y = 0} \hfill \\ {T \to T_{c} } \hfill & {at\;y = \infty } \hfill \\ \end{array} $$

(13)

Solution

The similarity conversions and dimensional variables which is utilized to change Eq. (11)– (13) in the set of ODE are considered byMajeed et al. [6] and Wang et al. [31,32,33,34,35,36].

$$ \begin{aligned} \eta & = \sqrt {\frac{c}{\nu }} y,\quad \xi = \sqrt {\frac{c}{\nu }} x,\quad u = cxf^{\prime } (\eta),\quad v = - \sqrt {cv} f(\eta) \\ \theta (\eta) & = \frac{{T - T_{\infty } }}{{T_{w} - T_{\infty } }} = \theta_{1} (\eta) + \xi^{2} \theta_{2} (\eta) \\ \end{aligned} $$

(14)

where in perspective of Eq. (14), the Eqs. (11)–(13) and the boundary conditions are converted to

$$ f^{\prime \prime \prime \prime } - (1 + \lambda_{2})(f^{\prime 2} - ff^{\prime \prime }) + \gamma_{1} (f^{\prime \prime 2} - ff^{iv}) - (1 + \lambda_{2})\frac{{2\beta \theta_{1} }}{{(\eta + \alpha_{1})^{4} }} + (1 + \lambda_{2})\theta_{1} Gr = 0 $$

(15)

$$ \theta_{1}^{\prime \prime } \left({1 + \frac{4}{3}R} \right) + \Pr (f\theta_{1}^{\prime } - 2f^{\prime } \theta_{1}) + \frac{{2\lambda \beta (\theta_{1} - \varepsilon)f}}{{(\eta + \alpha_{1})^{3} }} - 2\lambda f^{\prime 2} - Q\theta_{1} = 0 $$

(16)

$$ \theta_{2}^{\prime \prime } \left({1 + \frac{4}{3}R} \right) + \Pr (f\theta_{2}^{\prime } - 4f^{\prime } \theta_{1}) - 2\lambda \beta (\theta_{1} - \varepsilon)\left[{\frac{{f^{\prime } }}{{(\eta + \alpha_{1})^{4} }} + \frac{f}{{(\eta + \alpha_{1})^{5} }}} \right] + \frac{{2\lambda \beta \theta_{2} f}}{{(\eta + \alpha_{1})^{3} }} - \lambda f^{\prime \prime 2} - Q\theta_{2} = 0 $$

(17)

The boundary conditions (B.C.) are:

$$ \begin{aligned} & at\quad \eta = 0\quad \left\{ {f(\eta) = S - \,\frac{Me}{{\Pr }}\,\theta^{\prime } (\eta),\quad f^{\prime } (\eta) = 1 + Slip_{1} f^{\prime \prime } (\eta)} \right. \\ & at\quad \eta \to \infty \quad \left\{ {f \to 0,\quad f^{\prime \prime } \to 0} \right. \\ \end{aligned} $$

$$ \left\{ {\begin{array}{*{20}l} {\theta_{1} = 1,\quad \theta_{2} = 0\;for\;PST\;at\;\eta = 0} \hfill \\ {\theta_{1} \to 0,\quad \theta_{2} \to 0\;at\;\eta \to \infty } \hfill \\ \end{array} } \right. $$

(18)

"The skin friction coefficient Cf, local Nusselt number Nu_{x} and local Sherwood number Sh" are defined as

$$ C_{f} = \frac{{ - 2\tau_{w} }}{{\rho u_{w}^{2} }},\;Nu_{x} = q_{r} - \frac{{xq_{w} }}{{k(T_{c} - T_{w})}} $$

(19)

Here

$$ \tau_{w} = \left. {\left[{\mu \left({\frac{\partial u}{{\partial y}}} \right)} \right]} \right|_{y = 0} ,\;q_{w} = \left. { - \left({\frac{\partial T}{{\partial y}}} \right)} \right|_{y = 0} ;\;{\text{surface}}\;{\text{heat}}\;{\text{flux}} $$

(20)

On substituting value from Eq. (20) in to Eq. (19), we get thefollowing dimensionless expressions for skin friction coefficient, localNusselt number and local Sherwood number as given below:

$$ c_{f} {\text{Re}}_{x}^{\frac{1}{2}} = - 2f^{\prime \prime } $$

(21)

$$ \begin{aligned} Nu{\text{Re}}_{x}^{{\frac{ - 1}{2}}} & = - \left({1 + \frac{4}{3}R} \right)(\theta_{1}^{\prime } (0) + \xi^{2} \theta_{1}^{\prime } (0))\quad for\quad PST \\ Nu{\text{Re}}_{x}^{{\frac{ - 1}{2}}} & = - \left({1 + \frac{4}{3}R} \right)\frac{1}{{\left({\theta_{1} (0) + \xi^{2} \theta_{1} (0)} \right)}}\quad for\quad PHF \\ \end{aligned} $$

(22)

$Sh/\sqrt {\text{Re}} = - \phi^{\prime } (0),$ where ${\text{Re}} = ax^{2} /v$ local Reynolds number.

Result Discussion

In the current work, approximate solutions for the melting and permeable flows of a Jeffrey fluid over a linearly slip stretchysurface have been obtained by using R-K 4^{th}order shooting techniques. The motive of this object was to examine heat transfer and first-order slipy Jeffery fluid flow with magnetic dipole effect. We also investigated radiation with heat sources affecting past permeable linearly stretching or melting sheet. Various sets of the numerical solution have been accepted out for different mixtures of pertinent parameters namely, Various physical characteristics' effects ferromagnetic interaction parameter (β), Deborah number (γ), Radiation parameter (R), Heat sources parameter (Q),Prandtl number ($\Pr$), suction/injection parameter (S), ratio of relaxation to retardation times (λ_{2}) on velocity and temperature profiles is illustrated graphically with condition prescribed surface temperature (PST). It is also noted that Figs. 2, 3, 4, 5, 6, 7, 8, 9, 10, 11, 12, and 13 show that velocity as well as temperature profile with PST condition. By using the figures and tables, the impression of many relevant parameters is explored. The default parameter values for current work are considered as \(\lambda = 0.5\), \(\rho_{1} = 0.2\),\(\lambda_{2} = 0.1\),\(\Pr = 2,\,\,\beta = 0.2,\,\,\alpha_{1} = 1,\,\,\varepsilon = 2\),\(R = 1,\,\,Q = 1,\,\,Gr = 1,\,\,S = 0.5,\,\,Me = 0.5,\,\,Slip_{1} = 0.5\). By comparison of the numerical criterion of the Nusselt number by changing Pr in Table 1, the modified approach is proven to be accurate. The capability of the improved method is confirmed by this table. The absolute result of skin friction coefficient, Nusselt number in PST is given for numerical solution on permeable andmelting case for different data of physical parameter presented in Tables 2 and 3.

Fig. 2

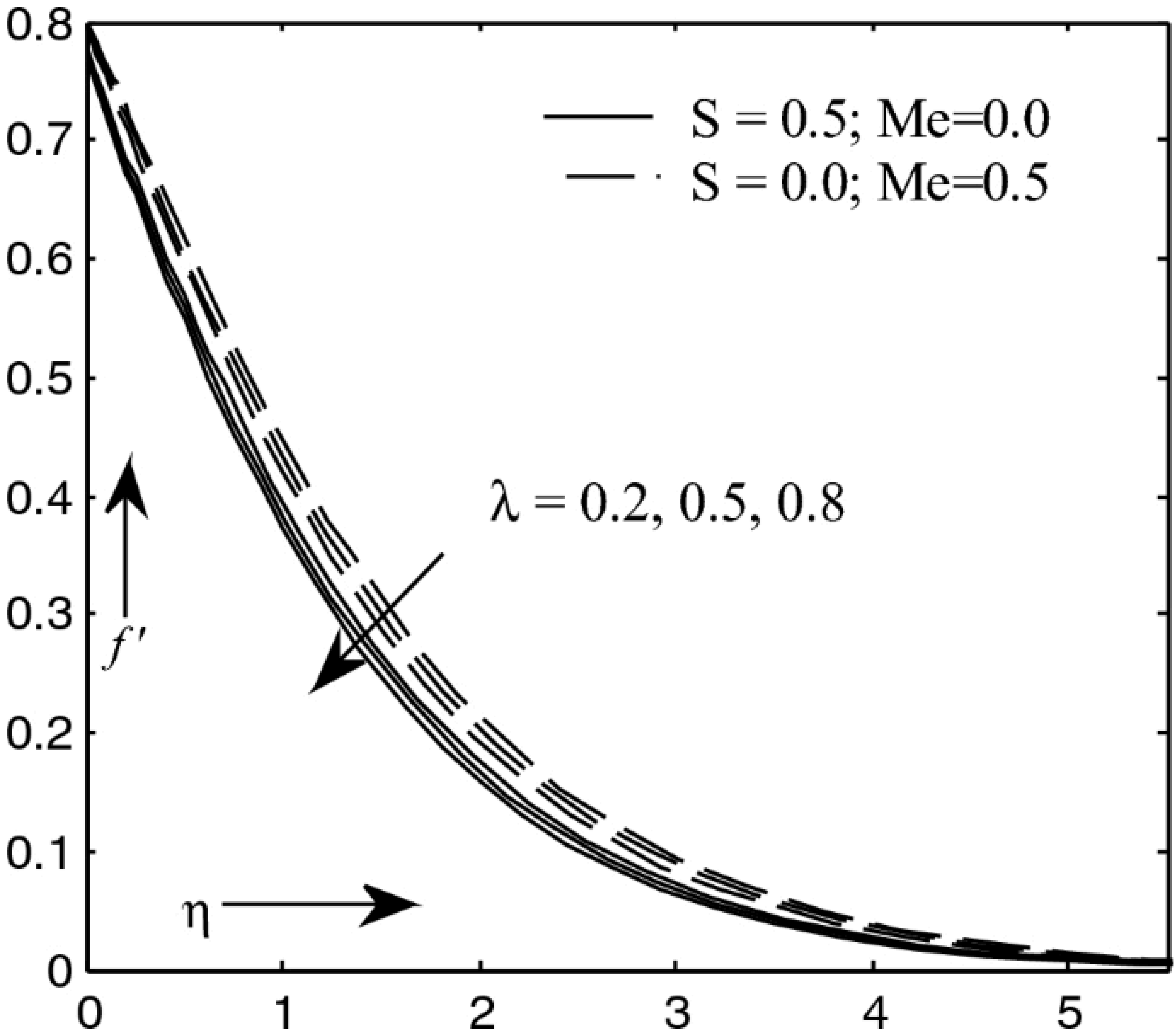

The influence of \(\lambda\) parameter on velocity

Fig. 3

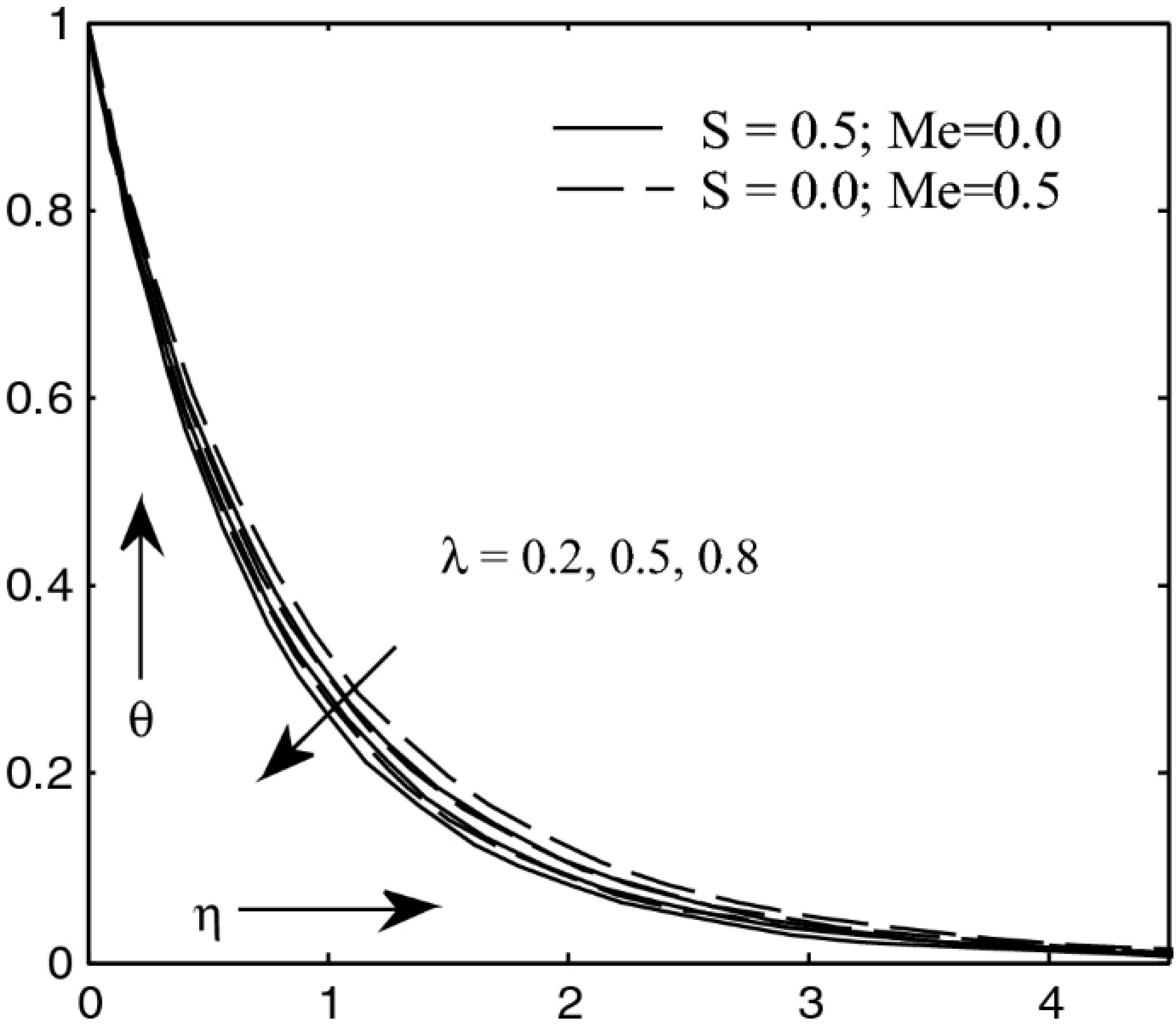

The influence of \(\lambda\) parameter on temperature

Fig. 4

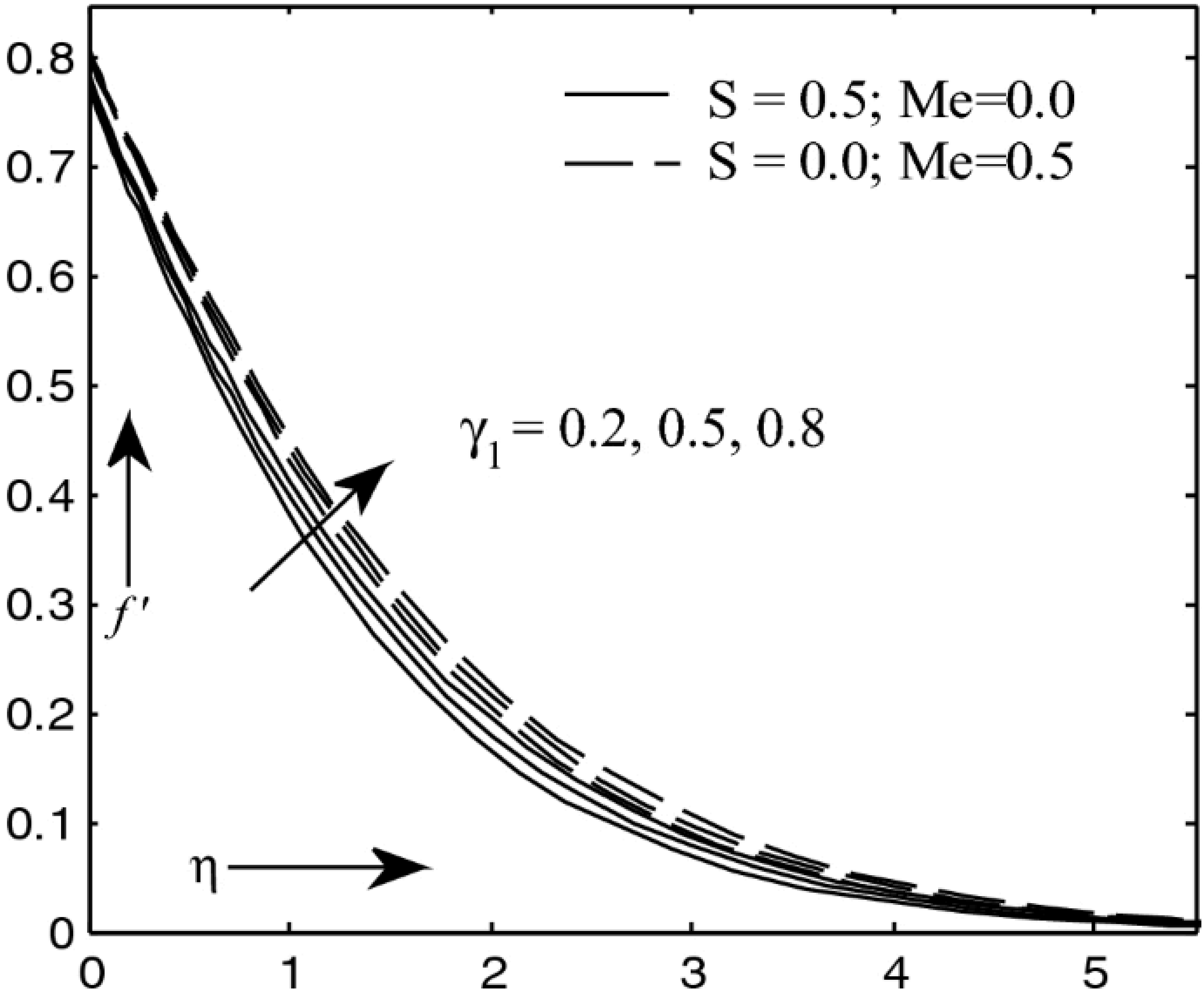

The influence of \(\gamma_{1}\) parameter on velocity

Fig. 5

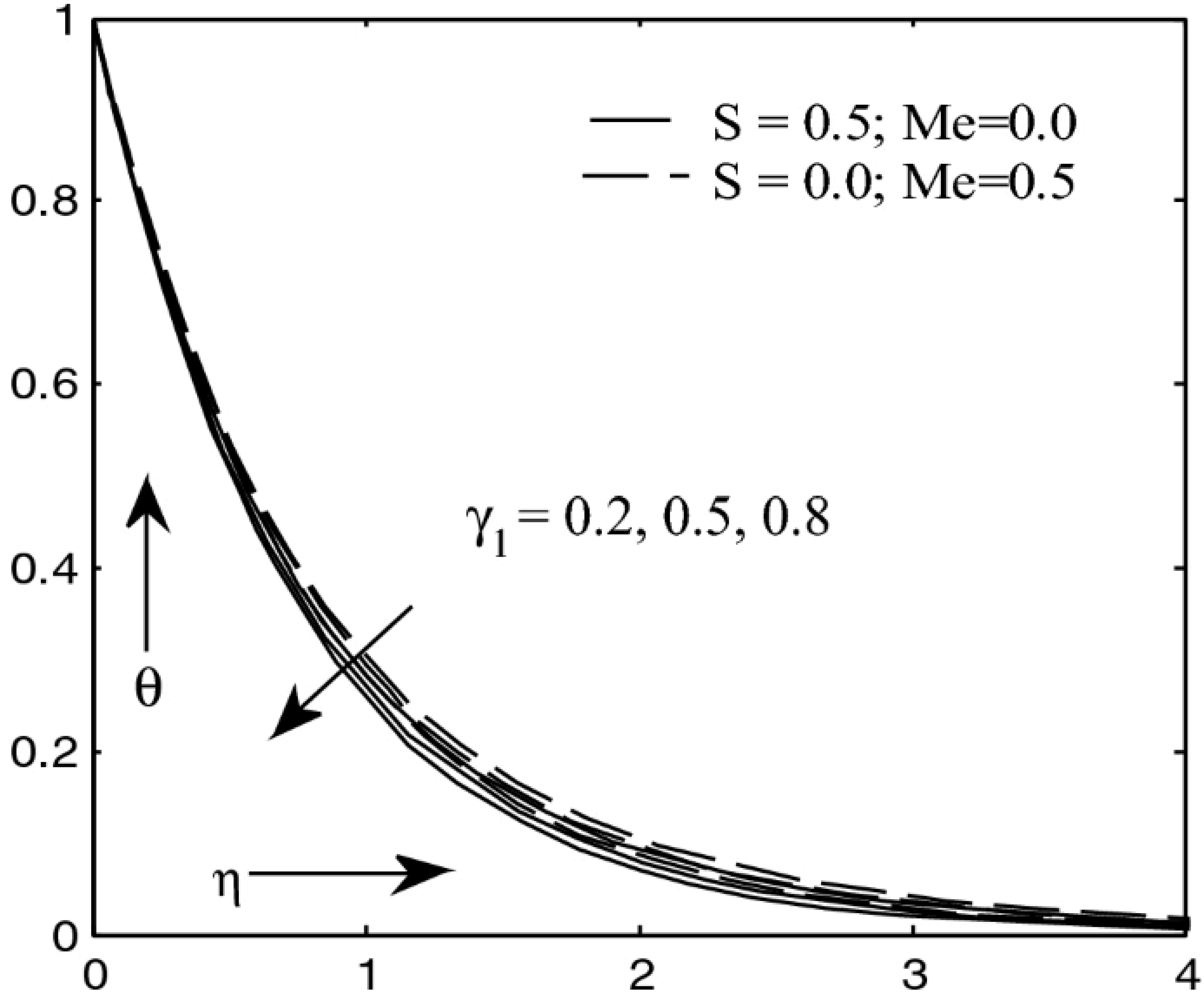

The influence of \(\gamma_{1}\) parameter on temperature

Fig. 6

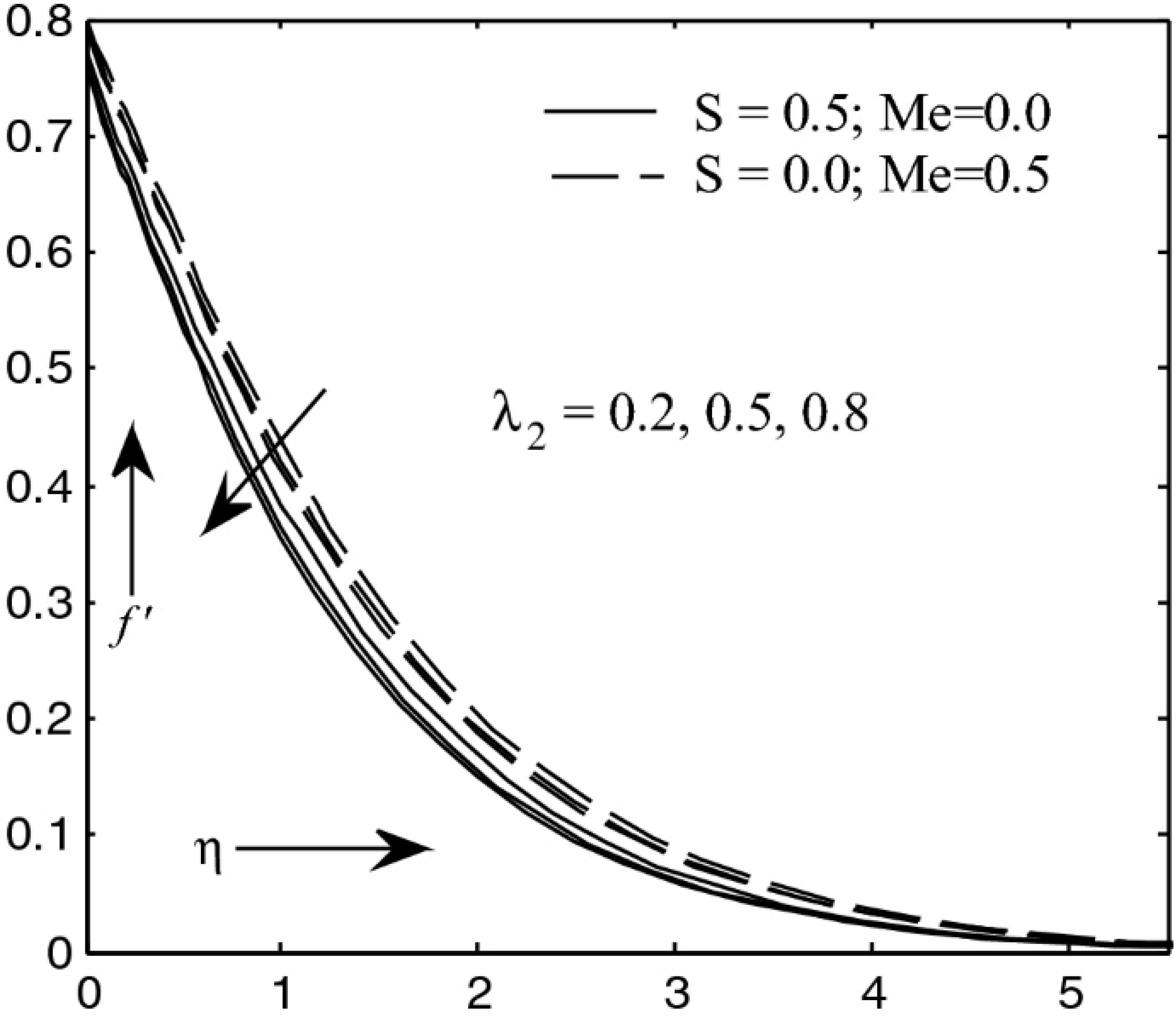

The influence of λ_{2} parameter on velocity

Fig. 7

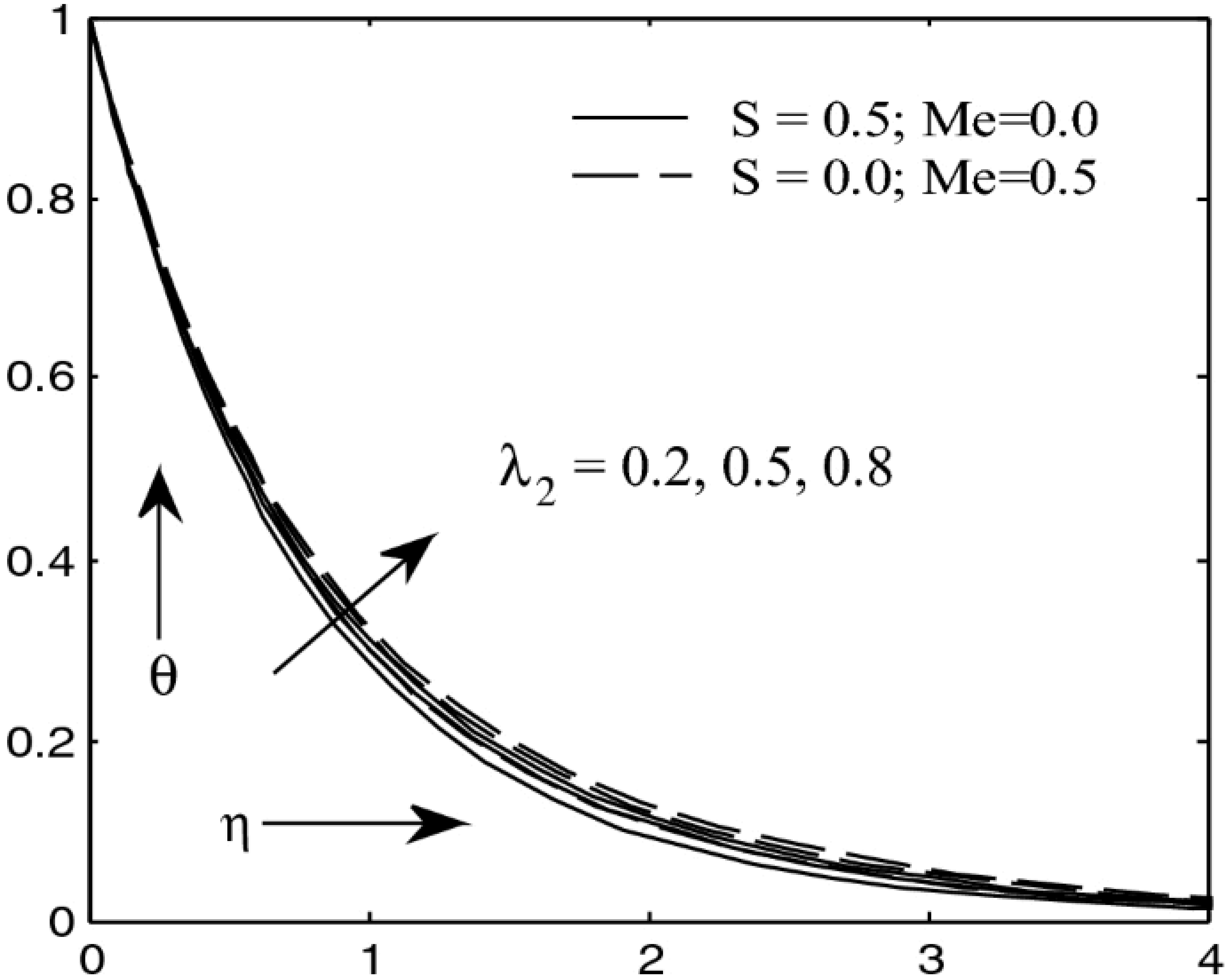

The influence of \(\lambda_{2}\) parameter on temperature

Fig. 8

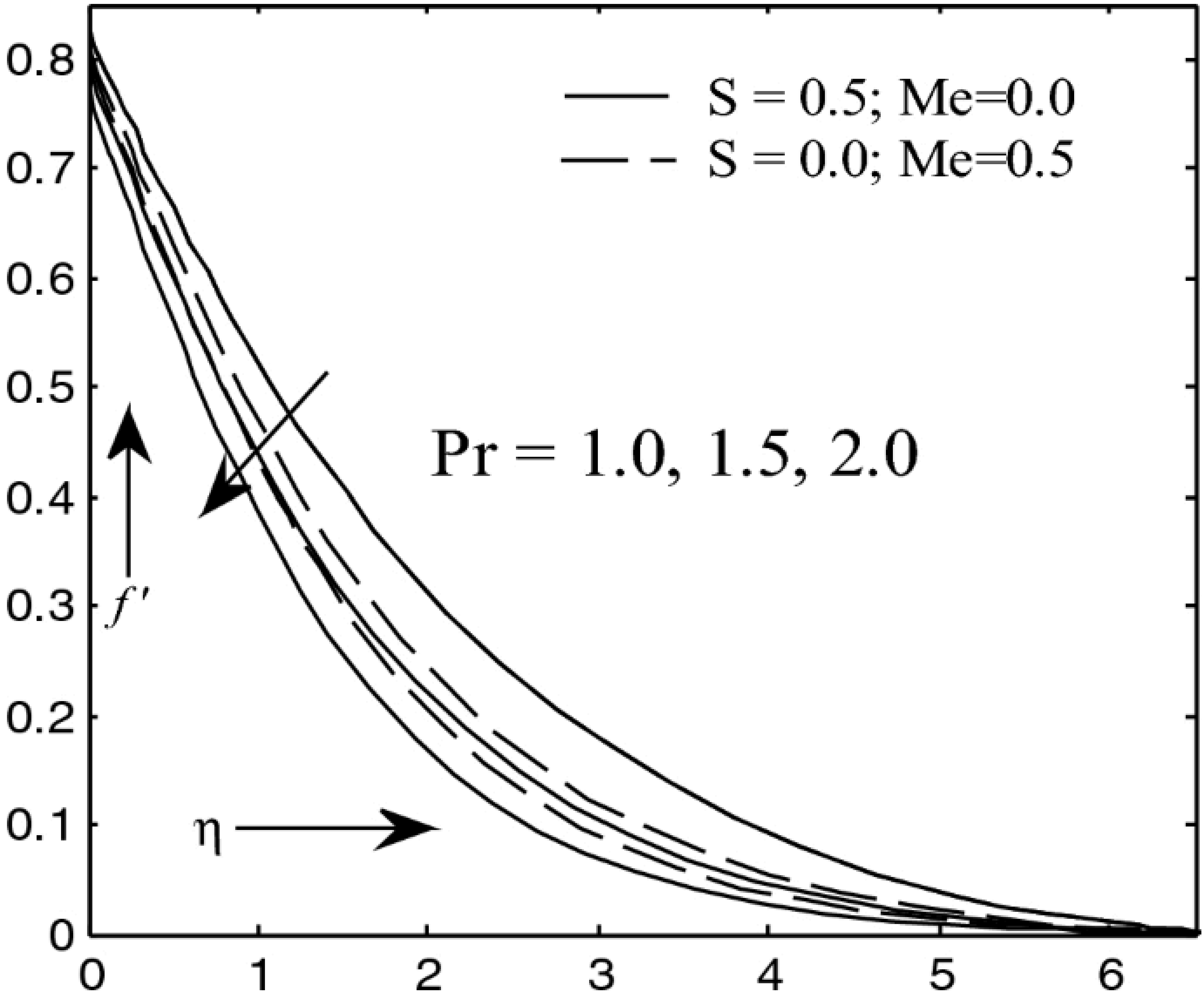

The influence of Pr parameter on velocity

Fig. 9

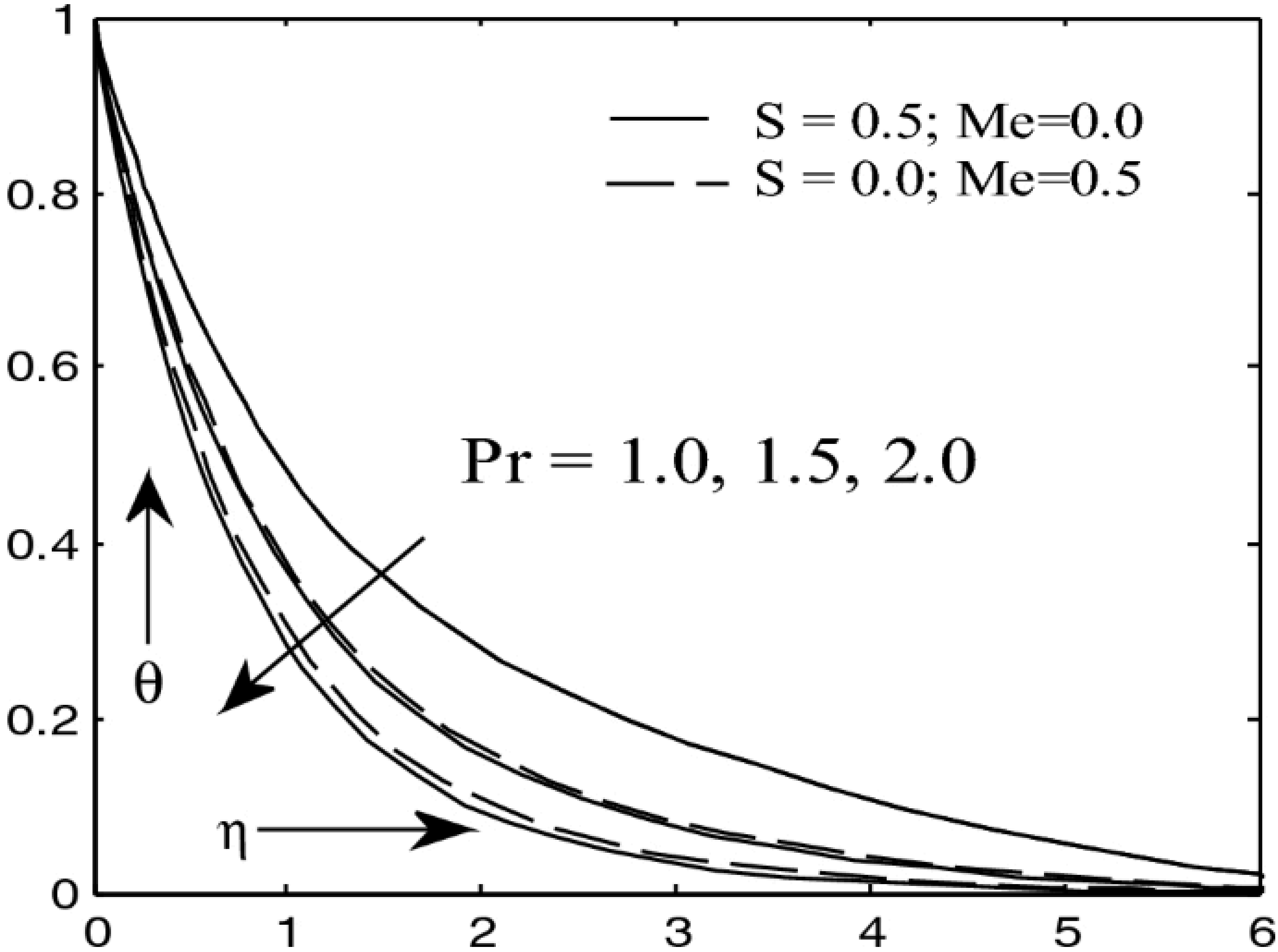

The influence of Pr parameter on temperature

Fig. 10

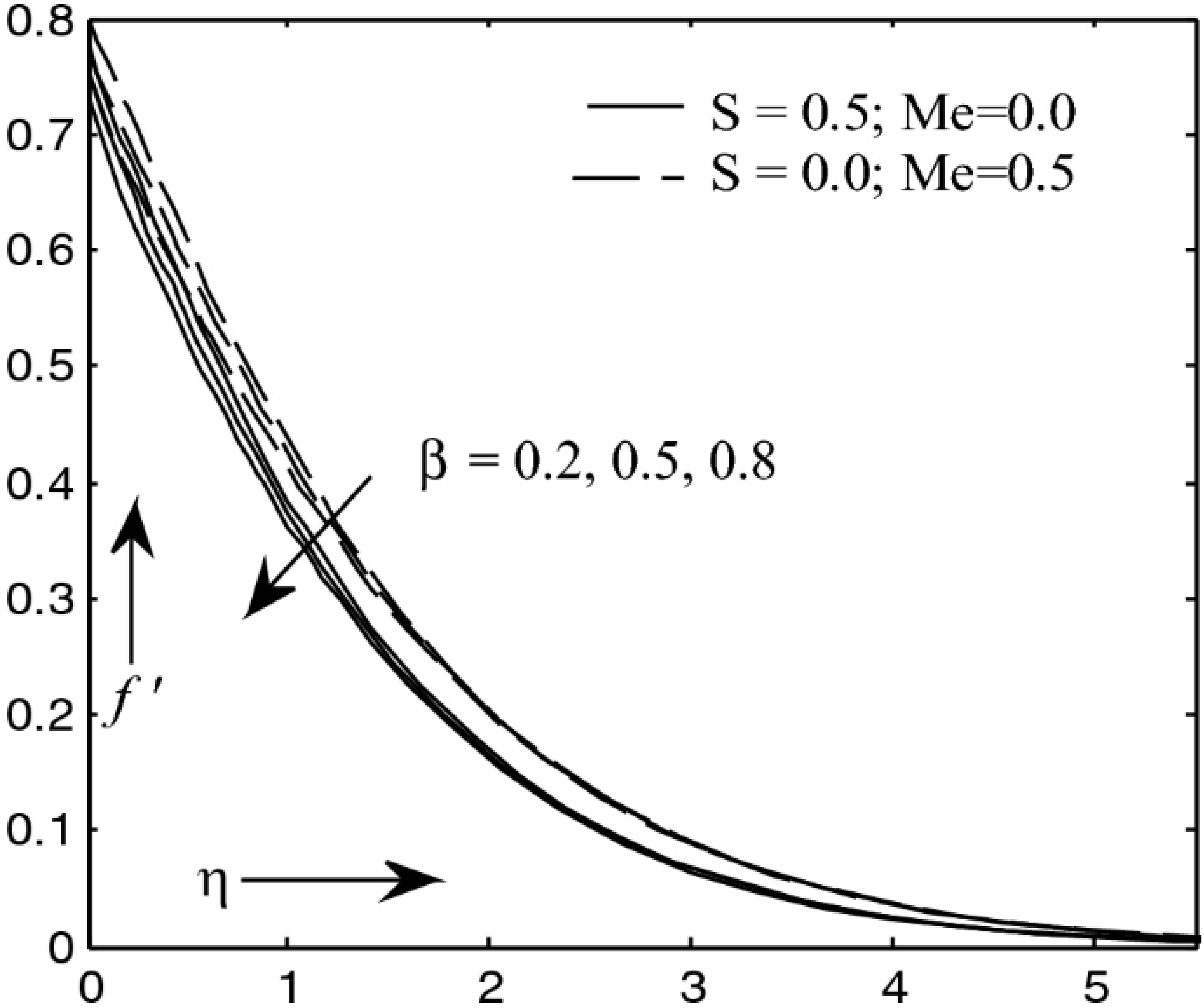

The influence of \(\beta\) parameter on velocity

Fig. 11

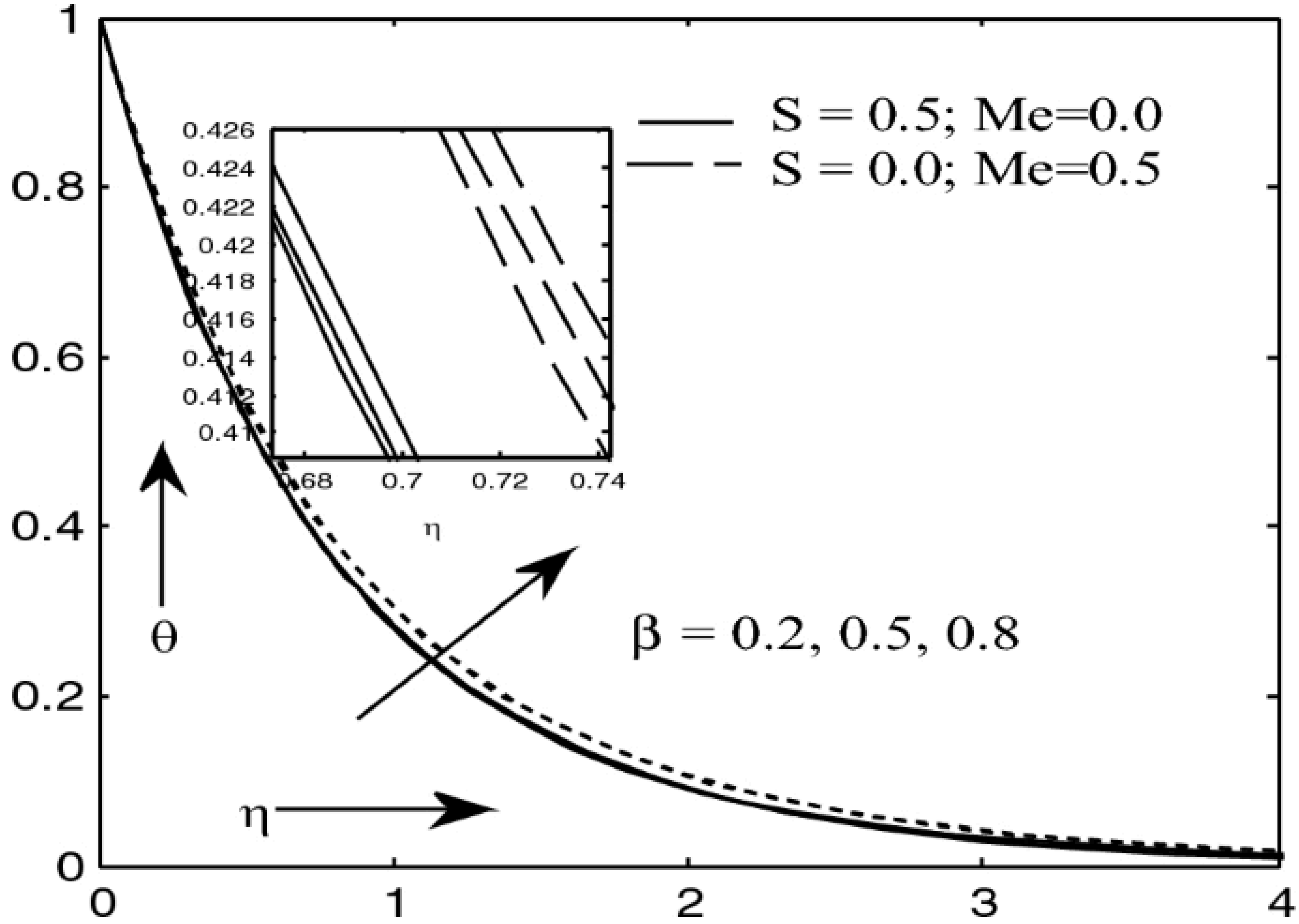

The influence of \(\beta\) parameter on temperature.

Fig. 12

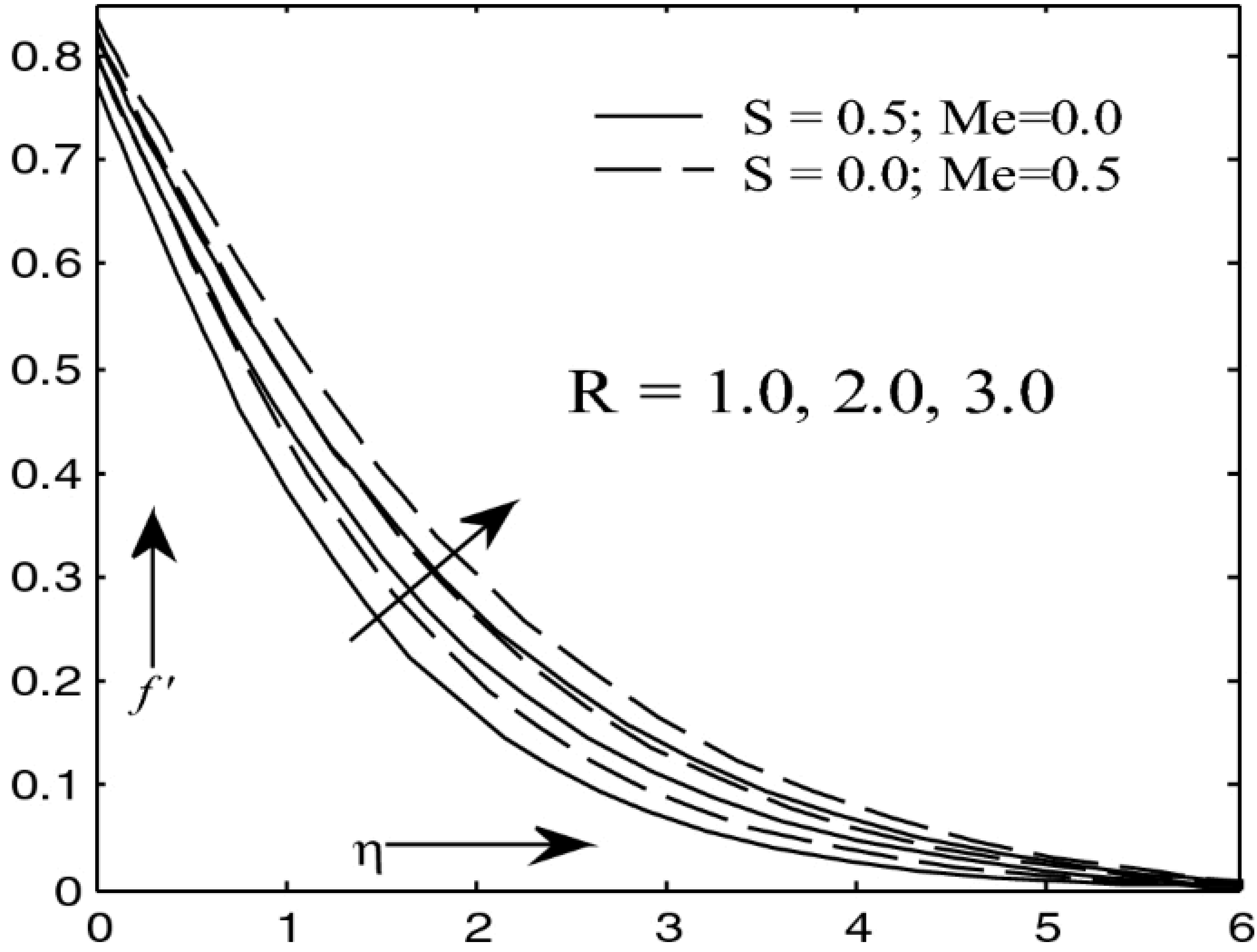

The influence of R parameter on velocity

Fig. 13

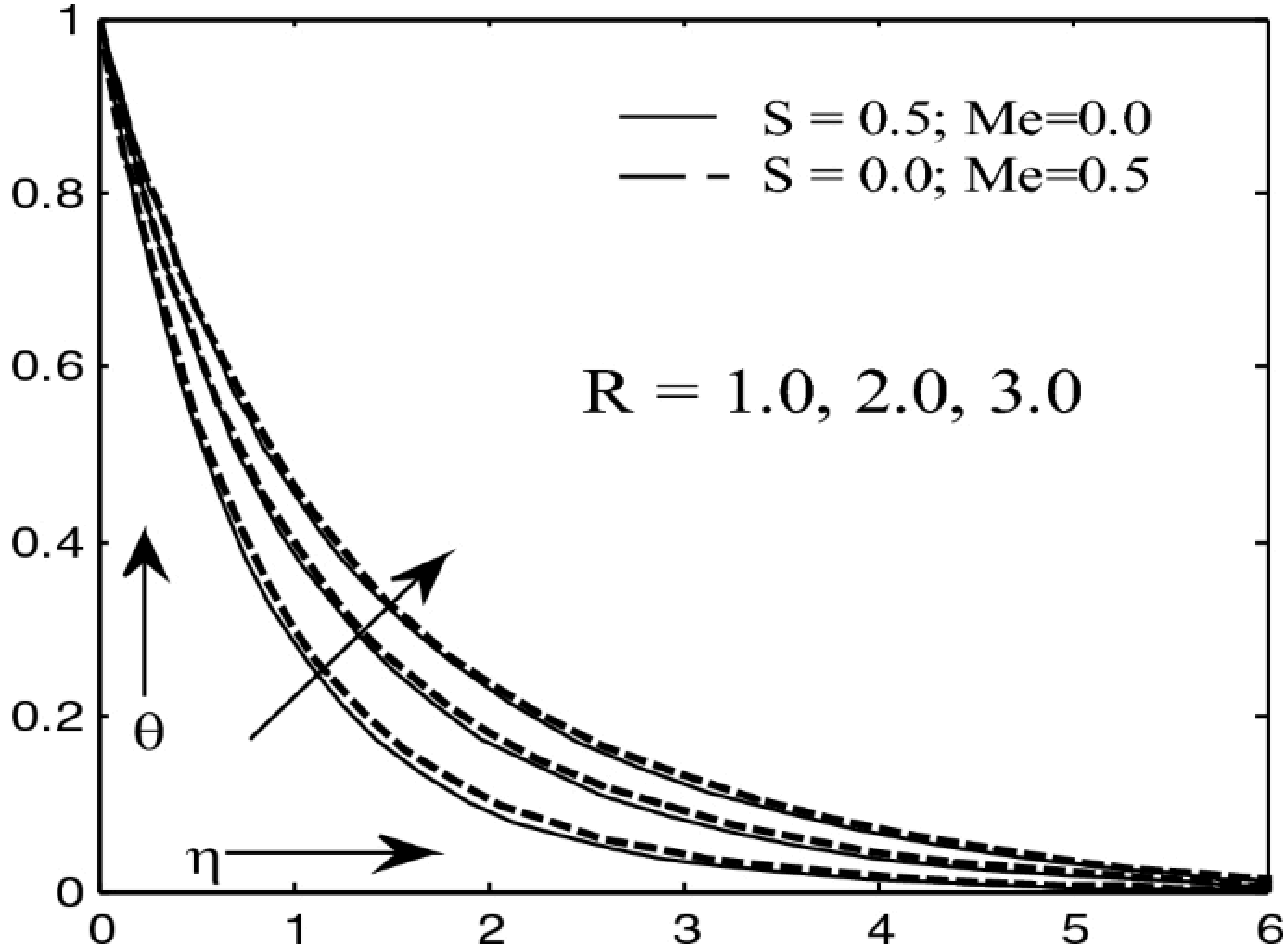

The influence of R parameter on temperature

Table 1 Comparison of Nusselt number \(- \theta_{1}{\prime} (0)\) for the value of \(\beta\) = 0, \(\lambda\) = 0, \(\lambda_{2}\) = 0, \(R\) = 0, \(\gamma_{1} = S = Q = Gr = 0\)

Table 2 The numerical values of skin friction coefficient (\(Cf\)), Nusselt number (\(Nu\)) in PST surface temperature is given for numerical solution on permeable surface case for various values of the physical parameter

Table 3 The numerical values of skin friction coefficient, Nusselt number in PST is given for numerical solution on melting surface case for various values of the physical parameter

The impression of the viscous dissipation parameter(λ) on temperature distribution as well as velocitycan be discovered in Figs. 2 and 3. It is noticed that velocity and temperature profiles get lower with the growth in the result λ. Physically, viscous dissipation occurs because the Jeffery fluid exhibits viscoelastic behavior, meaning that it possesses both viscous and elastic properties. As the fluid flows, the shear forces between adjacent layers cause energy to be transferred from the macroscopic motion of the fluid to the microscopic motion of its molecules. This energy is then dissolute as heat.The dissipation of energy results in a loss of kinetic energy within the fluid, leading to a decrement in velocity. Additionally, as energy is converted to heat, the fluid temperature increases. Consequently, both the velocity together with temperature profiles decrease as a conclusion of viscous dissipation.

Figures 4 and 5 exemplify the outcomes of Deborah's numbers γ_{1} on velocity $f^{\prime } \left(\eta \right)$, with temperature $\theta \left(\eta \right)$ profile. Whenever values of γ_{1} gets increased the velocity gets enhanced but alternatively temperature profile gets cut down. Physically, when a Jeffery fluid flows, it experiences viscous dissipation, which leads to the transformation of mechanical energy into heat due to internal friction within the fluid. This dissipation is more prominent at higher Deborah numbers when the elastic effects become significant. The fluid exhibits an increasingly noticeable elastic behavior as the Deborah number rises. This elastic behavior is associated with energy storage and release within the fluid, causing the temperature to be lower.

Figures 6 and 7 exhibit consequences of porosity parameter (λ_{2}) on velocity $f^{\prime } \left(\eta \right)$, with temperature $\theta \left(\eta \right)$ profile. Figure 6 showsflow stream reduces with improving meritsof the (λ_{2})parameter and on the other side effect seenon the temperature profile. Physically, the fluid flow is significantly announced with a growth in relaxation time (or decrease in retardation time) because growth in λ_{2} leads to rise in relaxation time; it means particles need much time to come back from the perturbed system to equilibrium system in which subsequently fluid velocity get lower.

Figures 8 and 9 show the impression of Prandtl number ($\Pr$) on velocity and temperature profiles. Increase the $\Pr$, and suppress the fluid velocity and thermal energy boundary layer thickness.$\Pr$ isthe ratio of momentum diffusivity to thermal diffusivity.Heat will diffuse from the sheet more quickly from fluids with lower inPr because they have high-level thermal conductivities.$\Pr$ may speed up the cooling process in conducting flows. The velocity together with the temperature profile plotted against the similarity variable (η) for distinct characteristics of the ferromagnetic interaction parameter(β) parameter is shown in Figs. 10 and 11. The figures indicate that with the rise in the parameter, the thickness of the momentum boundary layer decreases, while the temperature shows the opposite impact.

Figures 12 and 13 exemplify the significanceof radiation parameter (R) on velocity and temperature profile.From thesegraphs, it is noticeable that the momentum and thermal boundary layer thickness grows up with growth in the results of R. In general, as increases, the mean absorption coefficient falls, which causes the radiative heat flux to diverge. Resultant, the range of radiative heat transfer to the fluid rises, raising the fluid's temperature.

Conclusion

In the latest work, by utilizing R–K 4th order techniques approximate numerical results for the melting and permeable flow of Jeffrey fluid aroundstretchysurfaces have been derived. The motive of the research was to examineheat-transfer and first-order slipy Jeffery fluid flow with magnetic dipole effect. The investigation also revealed that the viscous dissipation parameter λ had counterintuitive effects on the thermal profile. Deborah numbers γ_{1} on velocity $f^{\prime } \left(\eta \right)$, with temperature $\theta \left(\eta \right)$ profile. Whenever values of γ_{1} gets increased the velocity gets enhanced but alternatively temperature profile gets cut down. In this article we find the tabulated form the numerical values of skin friction coefficient, Nusselt number in PST is given for numerical solution on melting surface case and without melting case for various values of the physical parameter. The two terms of flow have been explored. The impression of abundant quantities on velocity with temperature distribution is outlined as follows:

- The velocity $f^{\prime } \left(\eta \right)$ together with temperature $\theta \left(\eta \right)$, it noticed to rise with increasing amount of $\lambda \,$ and $\Pr$.
- The velocity $f^{\prime } \left(\eta \right)$ together with temperature $\theta \left(\eta \right)$ profile is higher for the melting boundary condition than permeable boundary condition.
- Meganetic field parameter and porosity parameter have propensity to reduce the skin friction coefficient (Cf) and local Nusselt number (Nu).
- Radiation parameter (R) has propensity to stand up the skin friction coefficient and local Nusselt number.

Data availability

This paper data not published any journal.

Abbreviations

a: Distance

c: Stretching rate $({\text{s}}^{ - 1})$

C_{p} **:** Specific heat at constant pressure

C_{f} **:** Skin friction coefficient

f **:** Dimensionless stream function

H **:** Magnetic field $({\text{A}}/{\text{m}})$

k **:** Thermal conductivity

K^{*} **:** Pyro magnetic coefficient

M: Magnetization $({\text{A}}/{\text{m}})$

κ: Extra stress tensor

N_{ux}: Local Nusselt number

$Pr = \frac{{\mu C_{p} }}{k}$: Prandtl number

Gr: Grashof number

θ: Dimensionless temperature

${\text{Re}}_{x} = \frac{{u_{w} x}}{v}$: Local Reynolds number

${\text{R}}_{1}$: Rivlin–Ericksen tensor

$S = \frac{{ - V_{w} }}{{\sqrt {cv} }}$: Suction/injection parameter

$R = \frac{{4\sigma T_{\infty }^{3} }}{3kk*}$: Radiation parameter

T: Temperature (K)

$Q = \frac{Q*}{{c\rho C_{p} }}$: Heat sources

T_{c}: Curie temperature (K)

(u,v): Velocity components $({\text{ms}}^{ - 1})$

(x,y): Coordinates along and normal to the sheet $({\text{m}})$

μ: Dynamic viscosity $({\text{N}}\,{\text{ms}}^{ - 1})$

μ_{0}: Magnetic permeability

$\alpha = a\sqrt{\frac{c}{v}}$: Dimensionless distance

$\beta = \frac{\gamma \rho }{2\pi \mu^{2} }\mu_{0} K^{*} (T_{c} - T_{w})$: Ferro magnetic interaction parameter

γ: Magnetic field strength $({\text{A}}/{\text{m}})$

$\gamma_{1} = \lambda_{1} c$: Deborah numbers

ρ: Density $({\text{kg}}\;{\text{m}}^{ - 3})$

$\varepsilon = \frac{T_{c} }{(T_{c} - T_{w})}$: Dimensionless curie temperature

(ξ ,η): Dimensionless coordinate

ψ: Stream function $({\text{m}}^{2} \;{\text{s}}^{ - 1})$

ϕ: Magnetic potential

τ: Cauchy stress tensor

$\lambda = \frac{c\mu^{2} }{\rho k(T_{c} - T_{w})}$: Viscous dissipation parameter

λ_{1} ,λ_{2}: Material parameters of Jeffrey's fluid

References

1. Ramesh, K.: Effects of viscous dissipation and Joule heating on the Couette and Poiseuille flows of a Jeffrey fluid with slip boundary conditions. Propuls. Power Res. **7**(4), 329–341 (2018)

Article Google Scholar

2. Abbas, S., Nazar, M., Nisa, Z.U., Amjad, M., Din, S.M.E., Alanzi, A.M.: Heat and mass transfer analysis of MHD Jeffrey fluid over a vertical plate with CPC fractional derivative. Symmetry **14**(12), 2491 (2022)

Article CAS ADS Google Scholar

3. Shehzad, S.A., Abdullah, Z., Alsaedi, A., Abbasi, F.M., Hayat, T.: Thermally radiative three-dimensional flow of Jeffrey nanofluid with internal heat generation and magnetic field. J. Magn. Magn. Mater. **397**, 108–114 (2016)

Article CAS ADS Google Scholar

4. Turkyilmazoglu, M., Pop, I.: Exact analytical solutions for the flow and heat transfer near the stagnation point on a stretching/shrinking sheet in a Jeffrey fluid. Int. J. Heat Mass Transf. **57**(1), 82–88 (2013)

Article Google Scholar

5. Ellahi, R., Rahman, S.U., Nadeem, S.: Blood flow of Jeffrey fluid in a catherized tapered artery with the suspension of nanoparticles. Phys. Lett. A **378**(40), 2973–2980 (2014)

Article CAS ADS Google Scholar

6. Ellahi, R., Hussain, F., Ishtiaq, F., Hussain, A.: Peristaltic transport of Jeffrey fluid in a rectangular duct through a porous medium under the effect of partial slip: an application to upgrade industrial sieves/filters. Pramana **93**, 1–9 (2019)

Article Google Scholar

7. Hayat, T., Iqbal, Z., Mustafa, M., Alsaedi, A.: Unsteady flow and heat transfer of Jeffrey fluid over a stretching sheet. Therm. Sci. **18**(4), 1069–1078 (2014)

Article Google Scholar

8. Ahmed, J., Shahzad, A., Khan, M., Ali, R.: A note on convective heat transfer of an MHD Jeffrey fluid over a stretching sheet. AIP Adv. **5**(11), 117117 (2015)

Article ADS Google Scholar

9. Ogulu, A., Amos, E.: Modeling pulsatile blood flow within a homogeneous porous bed in the presence of a uniform magnetic field and time-dependent suction. Int. Commun. Heat Mass Transf. **34**(8), 989–995 (2007)

Article Google Scholar

10. Alam, J., Murtaza, G., Tzirtzilakis, E., Ferdows, M.: Biomagnetic fluid flow and heat transfer study of blood with gold nanoparticles over a stretching sheet in the presence of magnetic dipole. Fluids **6**(3), 113 (2021)

Article CAS ADS Google Scholar

11. Seddeek, M.A.: Effects of radiation and variable viscosity on a MHD free convection flow past a semi-infinite flat plate with an aligned magnetic field in the case of unsteady flow. Int. J. Heat Mass Transf. **45**(4), 931–935 (2002)

Article Google Scholar

12. Turkyilmazoglu, M.: Exact analytical solutions for heat and mass transfer of MHD slip flow in nanofluids. Chem. Eng. Sci. **84**, 182–187 (2012)

Article CAS Google Scholar

13. Mukhopadhyay, S.: Slip effects on MHD boundary layer flow over an exponentially stretching sheet with suction/blowing and thermal radiation. Ain Shams Eng. J. **4**(3), 485–491 (2013)

Article Google Scholar

14. Raptis, A.: Effects of thermal radiation on the MHD flow past a vertical plate. J. Eng. Thermophys. **26**, 53–59 (2017)

Article CAS Google Scholar

15. Iyoko, M., Olajuwon, B.I.: Study on impact of magnetic dipole and thermal radiation on flow/heat transfer of Jeffery fluid over stretching sheet with suction/injection. J. Adv. Res. Fluid Mech. Thermal Sci. **104**(1), 65–83 (2023)

Article Google Scholar

16. Singh, K., Kumar, M.: Melting heat transfer in boundary layer stagnation point flow of MHD micropolar fluid towards a stretching/shrinking surface. JJMIE, **8**(6) (2014)

17. Hayat, T., Muhammad, K., Alsaedi, A., Asghar, S.: Numerical study for melting heat transfer and homogeneous-heterogeneous reactions in flow involving carbon nanotubes. Results Phys. **8**, 415–421 (2018)

Article ADS Google Scholar

18. Epstein, M., Cho, D.H.: Melting heat transfer in steady laminar flow over a flat plate. J. Heat Transf. **98**(3) (1976)

19. Ishak, A., Nazar, R., Bachok, N., Pop, I.: Melting heat transfer in steady laminar flow over a moving surface. Heat Mass Transf. **46**, 463–468 (2010)

Article ADS Google Scholar

20. Yacob, A., Ishak, A., Pop, I.: Melting heat transfer in boundary layer stagnation-point flow towards a stretching/shrinking sheet in a micropolar fluid. Comput. Fluids **47**, 16–21 (2011)

Article MathSciNet CAS Google Scholar

21. Olkha, A., Dadheech, A.: Second law analysis for radiative MHD slip flow for two different non-Newtonian fluid with Heat Source. J. Nanofluid. **10**(1), 447–461 (2021)

Article Google Scholar

22. Olkha, A., Dadheech, A.: Second law analysis for casson fluid flow over permeable surface embedded in porous medium. Nonlinear Stud. **28**(4), 1–13 (2021)

MathSciNet Google Scholar

23. Dadheech, P.K., et al.: Entropy analysis for radiative inclined MHD slip flow with heat source in porous medium for two different fluids. Case Stud. Thermal Eng. **28**, 101491 (2021)

Article MathSciNet Google Scholar

24. Dadheech, A., Parmar, A., Agrawal, K., Al-Mdallal, Q., Sharma, S.: Second law analysis for MHD slip flow for Williamson fluid over a vertical plate with Cattaneo-Christov heat flux. Case Stud. Therm. Eng. **33**, 101931 (2022)

Article Google Scholar

25. Labropulu, F., Husain, I., Chinichian, M.: Stagnation-point flow of the Walters' B'fluid with slip. Int. J. Math. Math. Sci. **2004**(61), 3249–3258 (2004)

Article MathSciNet Google Scholar

26. Ali, N., Khan, S.U., Sajid, M., Abbas, Z.: Slip effects in the hydromagnetic flow of a viscoelastic fluid through porous medium over a porous oscillatory stretching sheet. J. Porous Media **20**(3) (2017)

27. Govindarajan, A., Rajesh, K., Vidhya, M., Siva, E.P.: Effect of mass transfer and slip effect on viscoelastic fluid in a vertical channel with heat source and radiation. In: AIP Conference Proceedings (vol. 2112, no. 1, p. 020184). AIP Publishing LLC (2019)

28. Dawar, A., Saeed, A., Shah, Z., Kumam, W., Islam, S., Kumam, P.: Analytical simulation for magnetohydrodynamicmaxwell fluid flow past an exponentially stretching surface with first-order velocity slip condition. Coatings **11**(8), 1009 (2021)

Article CAS Google Scholar

29. Olkha, A., Dadheech, A.: Unsteady magneto hydro dynamic slip flow of Powell–Eyring fluid with microorganisms over an inclined permeable stretching sheet. J. Nanofluid. **10**(1), 128–145 (2021)

Article Google Scholar

30. Dadheech, A., Olkha, A., Parmar, A.: Inclined MHD and radiative Maxwell slip flow and heat transfer due to permeable melting surface with a non-linear heat source. Int. J. Appl. Comput. Math., **7**(89) (2021)

31. Wang, F., Asjad, M.I., Rehman, S.U., Ali, B., Hussain, S., Gia, T.N., Muhammad, T.: MHD Williamson nanofluid flow over a slender elastic sheet of irregular thickness in the presence of bioconvection. Nanomaterials **11**(9), 2297 (2021). https://doi.org/10.3390/nano11092297

Article CAS PubMed PubMed Central Google Scholar

32. Wang, F., Fatunmbi, E.O., Adeosun, A.T., Salawu, S.O., Animasaun, I.L., Sarris, I.E.: Comparative analysis between copper ethylene-glycol and copper-iron oxide ethylene-glycol nanoparticles both experiencing Coriolis force, velocity and temperature jump. Case Stud. Therm. Eng. 103028. https://doi.org/10.1016/j.csite.2023.103028

33. Wang, F., Saeed, A.M., Puneeth, V., Shah, N.A., Anwar, M.S., Geudri, K., Eldin, S.M.: Heat and mass transfer of Ag-H_2O nano-thin film flowing over a porous medium: a modified Buongiorno's model. Chin. J. Phys. (2023). https://doi.org/10.1016/j.cjph.2023.01.001

Article Google Scholar

34. Wang, F., Awais, M., Parveen, R., Alam, M.K., Rehman, S., Deif, A.M.H., Shah, A.N.: Melting rheology of three-dimensional Maxwell nanofluid (graphene-engine-oil) flow with slip condition past a stretching surface through Darcy–Forchheimer medium. Results Phys. **51**, 106647 (2023)

35. Wang, F., Fatunmbi, E.O., Adeosun, A.T., Salawu, S.O., Animasaun, I.L., Sarris, I.E. Comparative analysis between copper ethylene-glycol and copper-iron oxide ethylene-glycol nanoparticles both experiencing Coriolis force, velocity and temperature jump. Case Stud. Therm. Eng. 103028

36. Wang, F.Z., Asjad, M.I., Zahid, M., Iqbal, A., Ahmad, H., Alsulami, M.D.: Unsteady thermal transport flow of Cassonnanofluids with generalized Mittag–Leffler kernel of Prabhakar's type. J. Mater. Res. Technol. **14**, 1292–1300 (2021)

Article CAS Google Scholar

Funding

The authors have not disclosed any funding.

Author information

Authors and Affiliations

Department of Mathematics, Poornima University, Jaipur, India

Krishna Agarwal & Randhir Singh Baghel

Department of Mathematics, Arya College of Engineering, and I.T, Jaipur, India

Amit Parmar

Department of Mathematics, Swami Keshvanand Institute of Technology, Management and Gramothan, Jaipur, India

Amit Dadheech

Contributions

All author contribution to solve the problem and graphically represent. All author verify and examine the result and formulation.

Corresponding author

Correspondence to Amit Parmar.

Ethics declarations

Conflict of interest

The authors declare that they have no conflicts of interest.

Additional information

Publisher's Note

Rights and permissions

About this article

Cite this article

Agarwal, K., Baghel, R.S., Parmar, A. *et al.* Jeffery Slip Fluid Flow with the Magnetic Dipole Effect Over a Melting or Permeable Linearly Stretching Sheet. *Int. J. Appl. Comput. Math* **10**, 5 (2024). https://doi.org/10.1007/s40819-023-01629-w

Accepted
21 October 2023

Published
08 December 2023

DOI
https://doi.org/10.1007/s40819-023-01629-w

Share this article

Anyone you share the following link with will be able to read this content:

Get shareable link

Keywords

Jeffery fluid
Magnetic dipole
Melting
Slip flow
Permeable surface